

In presenting the dissertation as a partial fulfillment of the requirements for an advanced degree from the Georgia Institute of Technology, I agree that the Library of the Institute shall make it available for inspection and circulation in accordance with its regulations governing materials of this type. I agree that permission to copy from, or to publish from, this dissertation may be granted by the professor under whose direction it was written, or, in his absence, by the Dean of the Graduate Division when such copying or publication is solely for scholarly purposes and does not involve potential financial gain. It is understood that any copying from, or publication of, this dissertation which involves potential financial gain will not be allowed without written permission.

7/25/68

AXISYMMETRIC FREE TORSIONAL VIBRATIONS
OF A THICK, HOLLOWED, CONICAL FRUSTUM
CANTILEVERED AT THE SMALL END

A THESIS

Presented to

The Faculty of the Division of Graduate
Studies and Research

by

Surendra Ratilal Shah

In Partial Fulfillment

of the Requirements for the Degree
Master of Science in Engineering Mechanics

Georgia Institute of Technology

December, 1970

AXISYMMETRIC FREE TORSIONAL VIBRATIONS
OF A THICK, HOLLOWED, CONICAL FRUSTUM
CANTILEVERED AT THE SMALL END

Approved:

Chairman

Date approved by Chairman: 12-8-70

ACKNOWLEDGMENTS

The writer wishes to express his heartfelt gratitude to Dr. David J. McGill for creating interest in the problem, and providing guidance and encouragement throughout the preparation of this study. Appreciation is also due to Dr. M. E. Raviile, Director, School of Engineering Science and Mechanics, for his cheerful help in innumerable ways. Thanks are extended to Dr. J. T. S. Wang, a member of the examining committee, for his critical review of the manuscript and making excellent suggestions to enhance the value of this study. Mr. S. T. Chien provided invaluable help in writing computer programs. Credit is due to Mr. Cliff N. Wallace for drawing the superb illustrations and to Jackie Van Hook for typing this thesis.

TABLE OF CONTENTS

	Page
ACKNOWLEDGMENTS	ii
LIST OF TABLES	iv
LIST OF FIGURES	v
LIST OF SYMBOLS	vi
SUMMARY	viii
INTRODUCTION	1
SCOPE OF THE PROBLEM	3
FORMULATION OF THE PROBLEM	4
COORDINATE SYSTEM	7
BOUNDARY CONDITIONS	11
FINITE DIFFERENCE EQUATIONS	12
COMPUTATIONS	14
DISCUSSION OF RESULTS	19
RECOMMENDATIONS	32
APPENDIX A	33
APPENDIX B	36
APPENDIX C	40
BIBLIOGRAPHY	45

LIST OF TABLES

Table	Page
1. Comparison of Frequency Parameters at $\alpha = 90$ degrees . . .	18

LIST OF FIGURES

Figure	Page
1. Cone Geometry and Coordinate System	7
2. Grid Point Notation	12
3. Boundary Conditions for An Annular Circular Plate Fixed Along Its Inner Radius and Free Along Its Outer Radius . .	16
4. Frequency Parameter (Ψ) Vs. Cone Semivertex Angle (α) for Different Thickness Parameters (τ). Cone Completeness Parameter (K) = 0.50	22
5. Frequency Parameter (Ψ) Vs. Cone Semivertex Angle (α) for Different Thickness Parameters (τ). Cone Completeness Parameter (K) = 0.65	23
6. Frequency Parameter (Ψ) Vs. Cone Thickness Parameter (τ) for Different Cone Semivertex Angles (α). Cone Completeness Parameter (K) = 0.70	24
7. Frequency Parameter (Ψ) Vs. Cone Thickness Parameter (τ) for Different Cone Completeness Parameters (K). Cone Semivertex Angles (α) = 20, 50 and 90 Degrees	25
8. Frequency Parameter (Ψ) Vs. Cone Semivertex Angle (α) for Different Cone Completeness Parameters (K). Cone Thickness Parameters (τ) = 0.01, 0.20 and 0.50	26
9. Frequency Parameter (Ψ) Vs. Cone Completeness Parameter (K) for Different Semivertex Angles (α). Cone Thickness Parameter (τ) = 0.20	27
10. Frequency Parameter (Ψ) Vs. Cone Completeness Parameter (K) for Different Thickness Parameters (τ). Cone Semi- vertex Angle (α) = 50 Degrees	28
11. Torsional Mode Shapes for the Frustum of a Cone	29
12. Variation of the Normalized Displacements Along the Thick- ness of the Cone for the First Mode	30
13. Variation of the Normalized Displacements Along the Thick- ness of the Cone for the Second Mode	31
14. Coordinate System	33

LIST OF SYMBOLS

E	Modulus of elasticity or Young's modulus
h_r, h_s, h_θ	Lamé coefficients in r, s and θ directions respectively
S_T	Slant distance from apex of cone to fixed boundary of cone
S_0	Slant distance from apex of cone to free boundary of cone
s, r, θ	Coordinates in generatrix, inward normal and circumferential directions respectively
u_s, u_r, u_θ	Displacements in generatrix, inward normal and circumferential directions respectively
t	Time
T	Thickness
x, y, z	Cartesian coordinates
U	Strain energy of deformation
\vec{u}	Displacement vector
$\ddot{\vec{u}}$	Acceleration vector
α	Semivertex angle of cone
σ_{ij}	Stress tensor components
ϵ_{ij}	Strain tensor components
γ/S_0	Mesh size parameter in generatrix direction
δ/S_0	Mesh size parameter in thickness direction
$K = S_T/S_0$	Cone completeness parameter
λ	Lamé constant
μ	Lamé constant. Rigidity modulus or modulus of elasticity in shear

ν	Poisson's ratio
ρ	Mass density
τ	Thickness/ S_0 , Thickness parameter
ϕ	Strain energy of deformation per unit volume
$\Psi = \sqrt{\rho/\mu} \omega S_0$	Frequency parameter
ω	Circular frequency
$(\)$	$\frac{\partial(\)}{\partial t}$; t is time

Comma in subscript denotes differentiation

SUMMARY

It is known that for axisymmetric case, torsional modes of vibrations of cones are uncoupled from other modes of vibration. This simplifies the problem of axisymmetric torsional vibrations of cones; yet, little work has been done on the problem.

The axisymmetric free torsional vibrations of a thick, hollowed conical frustum which is cantilevered at the small end are studied. The limiting case of this is an annular plate fixed at the inner radius and free at the outer radius.

The basic vector equation of motion is transformed into three equations of motion in an orthogonal conical coordinate system. The equation for torsional motion is solved for eigenfrequencies using the finite difference technique. Thin shell theory predicts that the torsional frequencies are independent of semivertex angle. It is shown that the frequencies for thick cones increase with increase in semivertex angle. This rate of increase is greater for thick cones than for thin cones. However, frequencies are independent of thickness when semivertex angle is 90 degrees, i.e.; for the case an annular plate which is fixed at the inner radius and free at the outer radius. It is also shown that frequencies decrease as the cone approaches completeness. It is shown that the frequencies decrease with increasing thickness.

It is noted that the displacements are greater on outer face than for the inner face of the cone. However, the difference in displacements between the outer face and inner face decreases as semivertex angle

increases, and the displacements are constant throughout the thickness of the cone when the semivertex angle is 90 degrees, i.e.; for the limiting case of an annular plate.

INTRODUCTION

The frustum of a cone is used in wide-ranging applications such as aerospace vehicles, exhaust nozzles of jet engines and loud speakers. The emphasis on increased performance of aerospace vehicles, with minimum weight, has accelerated research in sophisticated methods of structural analysis. The goal of this emphasis is to alleviate or obviate structural failures in thin cones due to aerodynamic flutter and acoustic fatigue.

A shell can vibrate in the following modes or its combinations.

- (1) Extensional and Flexural (bending)
- (2) Torsional

Nash (1 and 2) has compiled bibliographies on the vibrations of cones, for the period prior to 1957, Hu (3) for the period 1957 through 1963. Gros and Forsberg (4) have also compiled a partially annotated bibliography on the subject covering the period from 1957 through March 1963. A review of the references listed in the above bibliographies and other literature (see, for example, references 5 through 18) show that the extensive theoretical and experimental research is done for the complex problem of extensional and flexural vibrations of a truncated cone. In contrast, the relatively simple problem of torsional vibrations of truncated conical shells has received little attention of researchers.

*Numerals in parentheses refer to the corresponding items in Bibliography.

The only significant work dealing with the subject is the result proved by Garnet, et al. (19) that the frequencies are independent of semivertex angle for the case of axisymmetric free torsional modes of vibrations of thin conical frustums. Then the natural question arises as to the behavior of thick conical frustums. It was also expected that the frequencies would decrease as the completeness of the cone increased. However, a gap in the knowledge exists about the effect of thickness, cone semivertex angle, or "conicity" and cone completeness on the axisymmetric free torsional vibrations of thick, hollowed truncated cones. This study examines the effect of these parameters on the axisymmetric free torsional vibrations of thick, hollowed conical frustum, which is cantilevered at the small end.

SCOPE OF THE PROBLEM

The effect of the following three parameters on the axisymmetric free torsional vibrational characteristics of a thick, hollowed conical frustum which is cantilevered at the small end, is found in this study:

- (1) Cone thickness parameter
- (2) Cone completeness parameter
- (3) Cone semivertex angle or "conicity"

The equation of motion for the axisymmetric torsional modes of free vibration is solved using the finite difference technique. The finite difference equations are solved by means of a high speed digital computer.

FORMULATION OF THE PROBLEM

The equations of motion are given by

$$\sigma_{ij,j} + X_i = \rho \ddot{u}_i ; \quad i = 1, 2, 3 \quad (1)$$

where

σ_{ij} = Stress tensor components

X_i = Externally applied body forces

$-\rho \ddot{u}_i$ = Inertia forces

ρ = Density of mass

u_i = Displacement components

Equation (1) can be transformed, as follows, to arrive at a system of three equations for the unknown displacements u_i .

Stress-deformation relationships are given by equation (B1) of Appendix B and is

$$\sigma_{ij} = 2\mu \epsilon_{ij} + \lambda \delta_{ij} e; \quad e = \epsilon_{kk} \quad (2)$$

in which

μ, λ Lamé constants

ϵ_{ij} Strain tensor components

$$\epsilon_{kk} = \sum_{i=1}^3 \epsilon_{ii}$$

$$\delta_{ij} \quad \text{Kronecker delta, i.e. } \delta_{ij} = \begin{cases} 1 & \text{for } i = j \\ 0 & \text{for } i \neq j \end{cases} .$$

The Lamé constants λ and μ are expressible as follows

$$\lambda = \frac{\nu E}{(1+\nu)(1-2\nu)} \quad \mu = \frac{E}{2(1+\nu)} \quad (3)$$

where

E = Young's modulus of elasticity

ν = Poisson's ratio.

The constant μ is also referred to as shear modulus or modulus of rigidity. Expressing the deformations in terms of displacements, i.e.

$$\epsilon_{ij} = \frac{1}{2} (u_{i,j} + u_{j,i}) \quad (4)$$

and using relationships of equation (2) and (4), equation (1) can be written as

$$\mu u_{i,jj} + (\lambda + \mu) u_{j,ji} + X_i = \rho \ddot{u}_i; \quad i = 1, 2, 3 \quad (5)$$

or, in vector form

$$\mu \nabla^2 \vec{u} + (\lambda + \mu) \text{grad div } \vec{u} + \vec{X} = \rho \ddot{\vec{u}} \quad (6)$$

since

$$\text{grad div } \vec{u} = \text{curl curl } \vec{u} + \nabla^2 \vec{u} . \quad (7)$$

Equation (6) can be represented in either of the following forms:

$$(\lambda+2\mu)\nabla^2\vec{u} + (\lambda+\mu)\text{curl curl } \vec{u} + \vec{X} = \rho\ddot{\vec{u}} \quad (8)$$

$$(\lambda+2\mu)\nabla(\nabla\cdot\vec{u}) - \mu\nabla\times(\nabla\times\vec{u}) + \vec{X} = \rho\ddot{\vec{u}} \quad (9)$$

For free vibrations, the term \vec{X} representing external force vector vanishes.

COORDINATE SYSTEM

The equations of motion given by (6), (8) and (9) are in vector form, and are independent of the coordinate system. The selection of the following orthogonal curvilinear system of coordinates simplifies the solution of the problem under consideration.

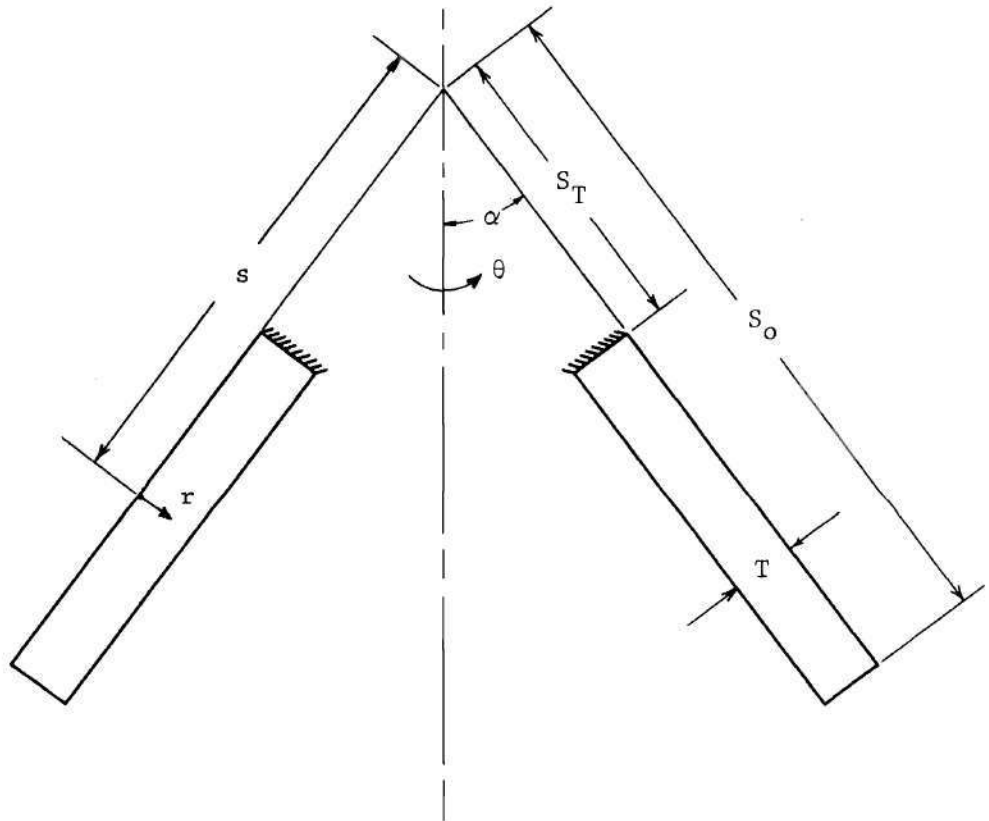


Figure 1 Cone Geometry and Coordinate System.

Two nondimensional parameters K (kappa) and τ (tau) are used

throughout this study. The parameter $K = \frac{S_T}{S_0}$ is the completeness of cone parameter ($0 < K < 1$). The cone is complete if $K = 0$ and is completely truncated if $K = 1$. The parameter $\tau = \frac{T}{S_0}$ is the cone thickness parameter, where T is the thickness of the cone ($0 < \tau \leq \infty$). Obviously, τ has an upper limit for any cone semivertex angle other than $\alpha = \frac{\pi}{2}$, this limit being governed by $\tau_{\max} = K \tan \alpha$.

The following three equations of motion in the (s, r, θ) coordinate system are obtained by using the relationships derived in Appendix A.

s Direction:

$$\begin{aligned} & \left(\frac{\lambda+2\mu}{\mu} \right) \left[u_{s,ss} + \left(\frac{\sin \alpha}{h_\theta} \right) u_{s,s} - \frac{\sin^2 \alpha}{h_\theta^2} u_s + \frac{\sin \alpha \cos \alpha}{h_\theta^2} u_r \right] \\ & - \left(\frac{\lambda+3\mu}{\mu} \right) \frac{\sin \alpha}{h_\theta^2} u_{\theta,\theta} + \left(\frac{\lambda+\mu}{\mu} \right) \left[\frac{u_{\theta,\theta s}}{h_\theta} - \left(\frac{\cos \alpha}{h_\theta} \right) u_{r,s} + u_{r,rs} \right] \\ & + u_{s,rr} + \frac{u_{s,\theta\theta}}{h_\theta^2} - \left(\frac{\cos \alpha}{h_\theta} \right) u_{s,r} = \frac{\rho}{\mu} \ddot{u}_s \end{aligned} \quad (10)$$

r Direction:

$$\begin{aligned} & \left(\frac{\lambda+2\mu}{\mu} \right) \left[u_{r,rr} - \left(\frac{\cos \alpha}{h_\theta} \right) u_{r,r} - \frac{\cos^2 \alpha}{h_\theta^2} u_r + \frac{\sin \alpha \cos \alpha}{h_\theta^2} u_s \right] \\ & + \left(\frac{\lambda+3\mu}{\mu} \right) \frac{\cos \alpha}{h_\theta^2} u_{\theta,\theta} + \left(\frac{\lambda+\mu}{\mu} \right) \left[\frac{u_{\theta,\theta r}}{h_\theta} + \left(\frac{\sin \alpha}{h_\theta} \right) u_{s,r} + u_{s,sr} \right] \\ & + u_{r,ss} + \frac{u_{r,\theta\theta}}{h_\theta^2} + \left(\frac{\sin \alpha}{h_\theta} \right) u_{r,s} = \frac{\rho}{\mu} \ddot{u}_r \end{aligned} \quad (11)$$

θ Direction:

$$\begin{aligned}
 & \left(\frac{\lambda+2\mu}{\mu} \right) \frac{u_{\theta,\theta\theta}}{h_\theta^2} + \left(\frac{\lambda+3\mu}{\mu} \right) \left[\left(\frac{\sin\alpha}{h_\theta^2} \right) u_{s,\theta} - \left(\frac{\cos\alpha}{h_\theta^2} \right) u_{r,\theta} \right] \\
 & + \left(\frac{\lambda+\mu}{\mu} \right) \left[\frac{u_{s,s\theta}}{h_\theta} + \frac{u_{r,r\theta}}{h_\theta} \right] + u_{\theta,ss} + u_{\theta,rr} + \left(\frac{\sin\alpha}{h_\theta} \right) u_{\theta,s} \\
 & - \left(\frac{\cos\alpha}{h_\theta} \right) u_{\theta,r} - \frac{u_\theta}{h_\theta^2} = \frac{\rho}{\mu} \ddot{u}_\theta . \quad (12)
 \end{aligned}$$

In the above equations,

$$h_\theta = s \sin\alpha - r \cos\alpha .$$

It is observed from the above equations that

(1) Equations in r direction can be obtained from equations in s direction by interchange of r and s and $\sin\alpha$, $\cos\alpha$ by $-\cos\alpha$, $-\sin\alpha$, respectively.

(2) Equations of motion in s and r directions are coupled for the case of axisymmetric vibrations.

Only the equation (12) is of interest for purely torsional vibrations. The terms involving derivatives with respect to θ drop out for the case of axisymmetric torsional vibrations and equation (12) is reduced to

$$u_{\theta,ss} + u_{\theta,rr} + \frac{\sin\alpha}{h_\theta} u_{\theta,s} - \frac{\cos\alpha}{h_\theta} u_{\theta,r} - \frac{u_\theta}{h_\theta^2} = \frac{\rho}{\mu} \ddot{u}_\theta . \quad (13)$$

It is noted that equation (13) for the axisymmetric torsional mode

of vibration is uncoupled from longitudinal and bending modes of vibration. This result is in agreement with the general result proved by Garnet, Goldberg and Salerno (19) that for the axisymmetric case, torsional modes of vibration are uncoupled from longitudinal and bending modes of vibration, for shells of revolution.

Assume the motion to be of form

$$u_{\theta}(s,r,t) = U_{\theta} e^{i\omega t} . \quad (14)$$

in which ω is the natural circular frequency of free vibration, and t is time. Then equation (13) can be time eliminated by use of relationship in equation (14) and is reduced to

$$s_o^2 \left[U_{\theta,ss} + U_{\theta,rr} + \frac{\sin\alpha}{h_{\theta}} U_{\theta,s} - \frac{\cos\alpha}{h_{\theta}} U_{\theta,r} - \frac{U_{\theta}}{h_{\theta}^2} \right] + \Psi^2 U_{\theta} = 0 . \quad (15)$$

Where

$$\Psi = \sqrt{\frac{\rho}{\mu}} \omega S_o$$

is a nondimensional frequency parameter.

BOUNDARY CONDITIONS

The boundary conditions for the problem are derived by variational procedure as shown in Appendix C. Only the boundary conditions shown in equations (C12) through (C14) is of interest for torsional vibrations. Also $\sigma_{\theta\theta} = 0$ for axisymmetric torsional vibrations. The boundary conditions for the problem of this thesis are

$$\begin{aligned}
 U_{\theta} &= 0 \text{ for } s = S_T \quad (\text{fixed edge}) \\
 \sigma_{s\theta} &= 0 \text{ for } s = S_o \quad (\text{free edge}) \\
 \sigma_{r\theta} &= 0 \text{ for } r = o \quad (\text{outer face}) \\
 \sigma_{r\theta} &= 0 \text{ for } r = t \quad (\text{inner face})
 \end{aligned} \tag{16}$$

For the axisymmetric case, stresses $\sigma_{s\theta}$ and $\sigma_{r\theta}$ in terms of displacements are obtained from equations in (B4) (see Appendix B), by dropping the terms involving derivatives with respect to θ , then,

$$\begin{aligned}
 \sigma_{\theta s} = \sigma_{s\theta} &= \mu \left(u_{\theta,s} - \frac{u_{\theta} \sin \alpha}{h_{\theta}} \right) \\
 \sigma_{r\theta} = \sigma_{\theta r} &= \mu \left(u_{\theta,r} + \frac{u_{\theta} \cos \alpha}{h_{\theta}} \right)
 \end{aligned} \tag{17}$$

FINITE DIFFERENCE EQUATIONS

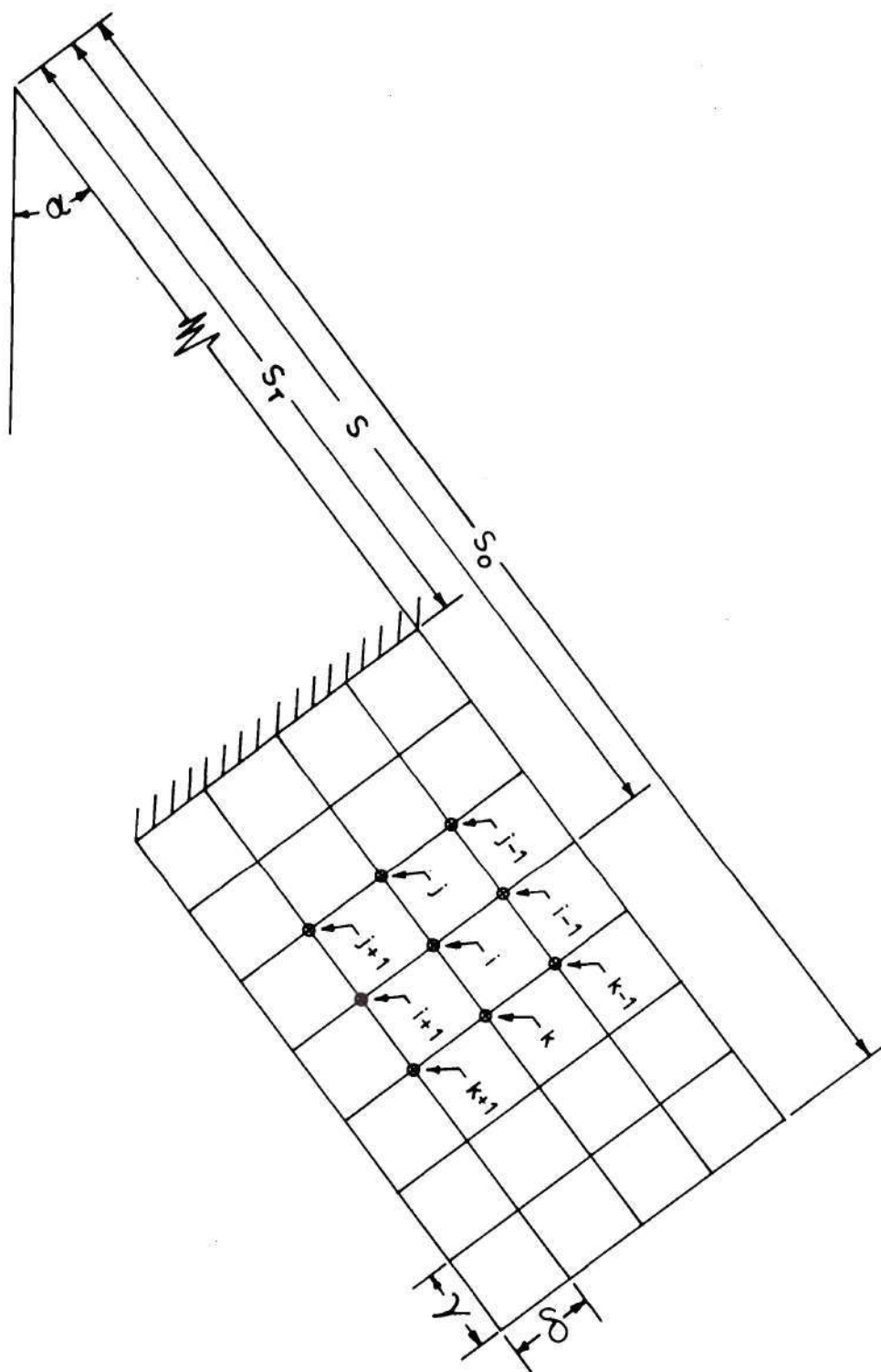


Figure 2 Grid Point Notation

Central differences, involving pivotal points symmetrically located with respect to the point under consideration, are more accurate than backward or forward differences. Hence equation (15), written in terms of central differences, becomes

$$\begin{aligned}
 & \frac{(U_\theta)_k - 2(U_\theta)_i + (U_\theta)_j}{\left(\frac{\gamma}{s_o}\right)^2} + \frac{(U_\theta)_{i+1} - 2(U_\theta)_i + (U_\theta)_{i-1}}{\left(\frac{\delta}{s_o}\right)^2} \\
 & + \frac{\sin\alpha}{\left(\frac{h_\theta}{s_o}\right)} \left[\frac{(U_\theta)_k - (U_\theta)_j}{\frac{2\gamma}{s_o}} \right] - \frac{\cos\alpha}{\left(\frac{h_\theta}{s_o}\right)} \left[\frac{(U_\theta)_{i+1} - (U_\theta)_{i-1}}{\frac{2\delta}{s_o}} \right] - \frac{(U_\theta)_i}{\left(\frac{h_\theta}{s_o}\right)^2} \\
 & + \psi^2 (U_\theta)_i = 0
 \end{aligned} \tag{18}$$

where γ and δ are the mesh sizes in generatrix and thickness directions respectively.

In computations square meshes are used i.e., $\gamma = \delta$, insuring that the errors involved in either direction are of the same order of magnitude.

COMPUTATIONS

The finite difference equations were programmed for solution by high speed digital computer. All computations were performed by the UNIVAC 1108 computer. Time limitations and memory capability of the computer limited the maximum size of the grid to 210 nodes.

The determination of eigenvalues of such a large matrix requires special care in selecting the computation method. It was observed that the coefficient matrix is nonsymmetric and "sparse", i.e., many of the coefficients were zero. In this particular problem, at most five elements in any row of the coefficient matrix are nonzero. Iteration methods are suitable for the solution of eigensystems of these types of matrices.

A large number of methods are available for the calculation of eigensystems of nonsymmetric matrices, but a high proportion of these are very unstable except for matrices of orders less than six. Some of the most stable methods are based on the reduction of the original matrix to upper Hessenberg form (i.e., to a matrix for which $a_{ij} = 0, i > j + 1$). Once the coefficient matrix is reduced to upper Hessenberg form, the Double Q-R algorithm developed by Francis (20) is a very effective method for determination of eigenvalues. Computer subroutines HSBG and ATEIG developed by IBM were used for reducing the original matrix to upper Hessenberg form and then determining the eigenvalues. Another advantage in reducing the unsymmetric matrix to upper Hessenberg form is the reduction by a factor of order N (N is the size of the matrix) in the number of computations required in the Double Q-R algorithm.

An excellent independent check on finite difference equations and estimate of error involved in computations of eigenfrequencies is performed in the following manner.

Equations of elastic motion in polar cylindrical coordinates (r, θ, z) are given in (22).

For torsional vibrations only the equation in θ direction is of interest and is,

$$\begin{aligned}
 (\lambda + 2\mu) & \left[\frac{1}{r} u_{r,r\theta} + \frac{1}{r^2} u_{r,\theta} + \frac{1}{r^2} u_{\theta,\theta\theta} + \frac{1}{r^2} u_{z,\theta z} \right] \\
 & - \mu \left[\frac{1}{r} u_{z,\theta z} - u_{\theta,zz} + \frac{1}{r^2} u_{\theta} - \frac{1}{r} u_{\theta,r} - u_{\theta,rr} + \frac{1}{r} u_{r,r\theta} - \frac{1}{r^2} u_{r,\theta} \right] \\
 & = \rho \ddot{u}_{\theta} .
 \end{aligned} \tag{19}$$

If motion in only the θ direction is considered, then

$$u_r = u_z = 0 .$$

Assuming harmonic motion

$$u_{\theta}(r, t) = U_{\theta}(r) e^{i\omega t} . \tag{20}$$

Equation (19) is simplified and rearranged to

$$r^2 U_{\theta,rr} + r U_{\theta,r} + U_{\theta} \left(\frac{\rho}{\mu} \omega^2 r^2 - 1 \right) = 0 . \tag{21}$$

The change of variable $R = \sqrt{\frac{\rho}{\mu}} \omega r$ in equation (21) leads to

$$R^2 \frac{d^2 U_\theta}{dR^2} + R \frac{dU_\theta}{dR} + U_\theta (R^2 - 1) = 0 . \quad (22)$$

This is Bessel's equation of order 1.

Also note that equations (21) and (22) are independent of z coordinate.

The general solution is given by

$$U_\theta = C_1 J_1(R) + C_2 Y_1(R) \quad (23)$$

or

$$U_\theta = C_1 J_1\left(\sqrt{\frac{\rho}{\mu}} \omega r\right) + C_2 Y_1\left(\sqrt{\frac{\rho}{\mu}} \omega r\right) . \quad (24)$$

Where

C_1, C_2 = Constants to be determined from boundary conditions.

J_1 = Bessel function of first kind and order 1.

Y_1 = Neumann's Bessel function of second kind and order 1.

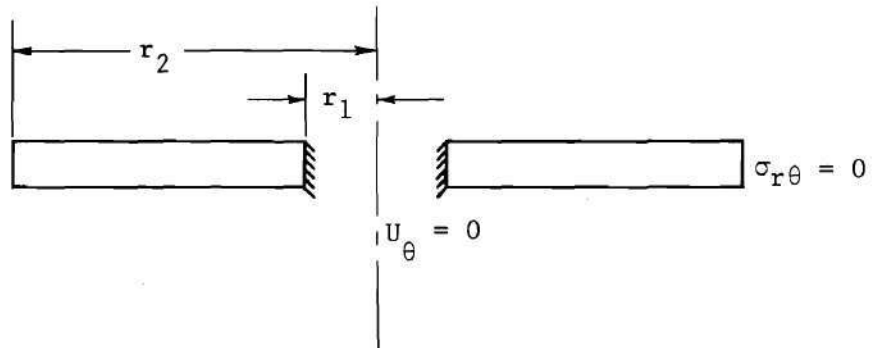


Figure 3. Boundary Conditions for An Annular Circular Plate Fixed Along its Inner Radius and Free Along Its Outer Radius.

Boundary conditions for an annular circular plate fixed along its inner radius and free along its outer radius are

$$\left. \begin{aligned} U_{\theta} &= 0 \quad \text{for } r = r_1 \\ \sigma_{r\theta} &= \mu \left[\frac{dU_{\theta}}{dr} - \frac{U_{\theta}}{r} \right] = 0 \quad \text{for } r = r_2 \end{aligned} \right\} . \quad (25)$$

or

$$\sigma_{r\theta} = \mu \left[\frac{dU_{\theta}}{dR} - \frac{U_{\theta}}{R} \right] = 0 \quad \text{for } r = r_2$$

Substitution of the boundary conditions, shown in (25), into equation (24), gives two homogeneous equations as follows

$$C_1 J_1 \left(\sqrt{\frac{\rho}{\mu}} \omega K \right) + C_2 Y_1 \left(\sqrt{\frac{\rho}{\mu}} \omega K \right) = 0 \quad (26)$$

$$C_1 J_2 \left(\sqrt{\frac{\rho}{\mu}} \omega \right) + C_2 Y_2 \left(\sqrt{\frac{\rho}{\mu}} \omega \right) = 0 \quad (27)$$

J_2 = Bessel function of first kind and order 2.

Y_2 = Neumann's Bessel function of second kind and order 2.

The determinant of coefficients of C_1 and C_2 in equations (26) and (27) should be zero for the nontrivial solution of equation (22), i.e.,

$$J_1 \left(\sqrt{\frac{\rho}{\mu}} \omega K \right) Y_2 \left(\sqrt{\frac{\rho}{\mu}} \omega \right) - J_2 \left(\sqrt{\frac{\rho}{\mu}} \omega \right) Y_1 \left(\sqrt{\frac{\rho}{\mu}} \omega K \right) = 0 . \quad (28)$$

The correctness of the computer program is established if the frequencies computed from equation (18), using the boundary conditions shown in equation (16) are independent of thickness at the semivertex angle of 90 degrees. Figures 4 through 8 show that frequencies are

indeed independent of thickness at the semivertex angle of 90 degrees and depend only on the cone completeness.

Table 1 shows the comparison of the first two computed eigenfrequencies with the exact eigenfrequencies obtained by solving equation (28) for different cone completeness parameters K .

Table 1. Comparison of Frequency Parameters at $\alpha = 90$ Degrees.

$\begin{array}{c} \Psi \\ K \end{array}$	First Mode		Second Mode	
	Present Work	Exact	Present Work	Exact
0.10	0.28739	0.28658	5.33096	5.33119
0.20	0.59568	0.59563	5.82426	5.82473
0.30	0.95250	0.95238	6.57520	6.57623
0.40	1.39210	1.39200	7.64130	7.64290
0.50	1.97320	1.97317	9.17450	9.17746
0.60	2.81029	2.80983	11.50748	11.50884
0.70	4.16531	4.16500	15.41460	15.41832
0.80	6.82512	6.82501	23.24675	23.25961
0.90	14.71645	14.71744	46.78564	46.81221

DISCUSSION OF RESULTS

The significant results of the computations are plotted in Figures 4 through 13.

1. Figures 4 and 5 show the influence on frequency of cone thickness and semivertex angle.

It is noted that frequency increases with increase in cone semivertex angle if the cone completeness parameter and thickness parameter are constant. This can be attributed to increase in inertia of the cone; for as semivertex angle increases with all else held constant, the inertia of mass elements increases. The rate of increase of frequency with increase in semivertex angle is greater for thick cones than for thin cones. However, frequencies are seen in Figures 4 through 8 to be independent of thickness at the semivertex angle of 90 degrees, as was shown earlier. Figures 4 through 8 all show that frequency decreases with increases in cone thickness. This can be explained by the fact that the stress $\sigma_{r\theta}$, acting across the cone thickness has a retarding effect on frequency, and the thicker the cone, the greater this effect will be. Also, frequency tends to be independent of semivertex angle as the cone approaches thin shell theory range, as can be seen in Figures 4 through 8. This result is in agreement with general result proved by Garnet, Goldberg and Salerno (19) that the natural frequencies of axisymmetric torsional motions are independent of semivertex angle for thin cones of revolution. The present results show that significant errors result at small semivertex angles if thin shell theory is used for computing

frequencies of thick cones.

2. Figures 9 and 10 show the effect on frequency of cone completeness parameter for constant thickness parameter and constant semivertex angle. It is observed that frequency increases with decrease in cone completeness, if thickness parameter and semivertex angle are constant. The same conclusion can be derived from Figures 7 and 8. This was expected since as $K \rightarrow 1$, the cone approaches a ring of rectangular cross section, fixed on one of its four faces, which is much stiffer than a nearly complete cone. Note that the cone is complete if $K = 0$ and is completely truncated if $K = 1$. It is observed that semivertex angle or thickness does not have an appreciable effect for short cones, i.e., those with K near unity.

Figure 9 shows that, for semivertex angle equal to 90 degrees, the frequency approaches zero as cone approaches completeness. In other words, frequencies approach zero as an annular circular plate approaches solid circular plate. This means that only rigid body motion is possible for a solid circular plate. This is due to decrease in an annular area resisting the motion as an annular plate approaches solid plate.

3. The first three mode shapes using the normalized midsurface displacements are plotted in Figure 11. The displacements are normalized with respect to the largest displacement occurring on the outer face of the cone. The normalized displacements for the outer face, midsurface and inner face are shown in Figures 12 and 13 for the first two natural modes of vibration. The displacements for the outer face, as expected, are larger than those of the inner face. However, it was noted that the difference in displacements between the outer face and inner face

decreases with increase in semivertex angle. The displacements are constant throughout the thickness of the cone when the semivertex angle is 90 degrees; this is equivalent to the case of an annular circular plate fixed at the inside radius and free at the outside radius.

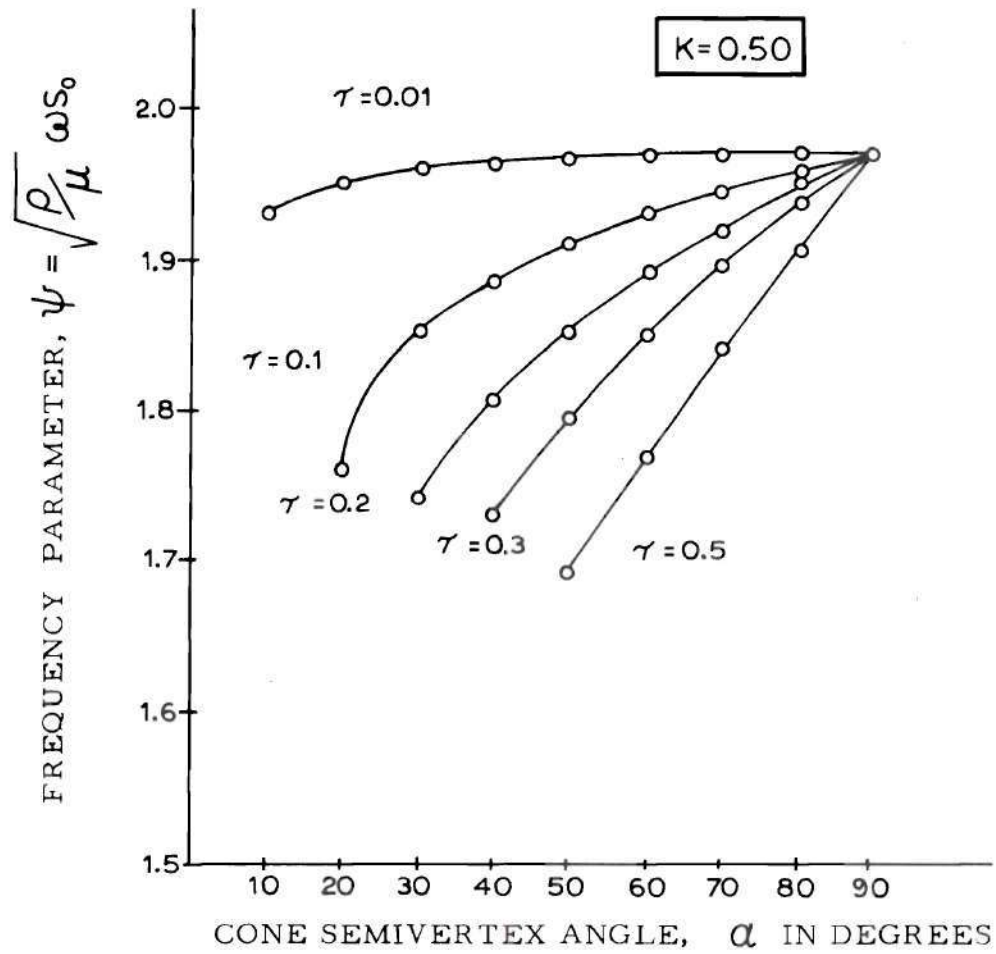


Figure 4 Frequency Parameter (ψ) Vs. Cone Semivertex Angle (α) For Different Thickness Parameters (τ). Cone Completeness Parameter (K) = 0.50

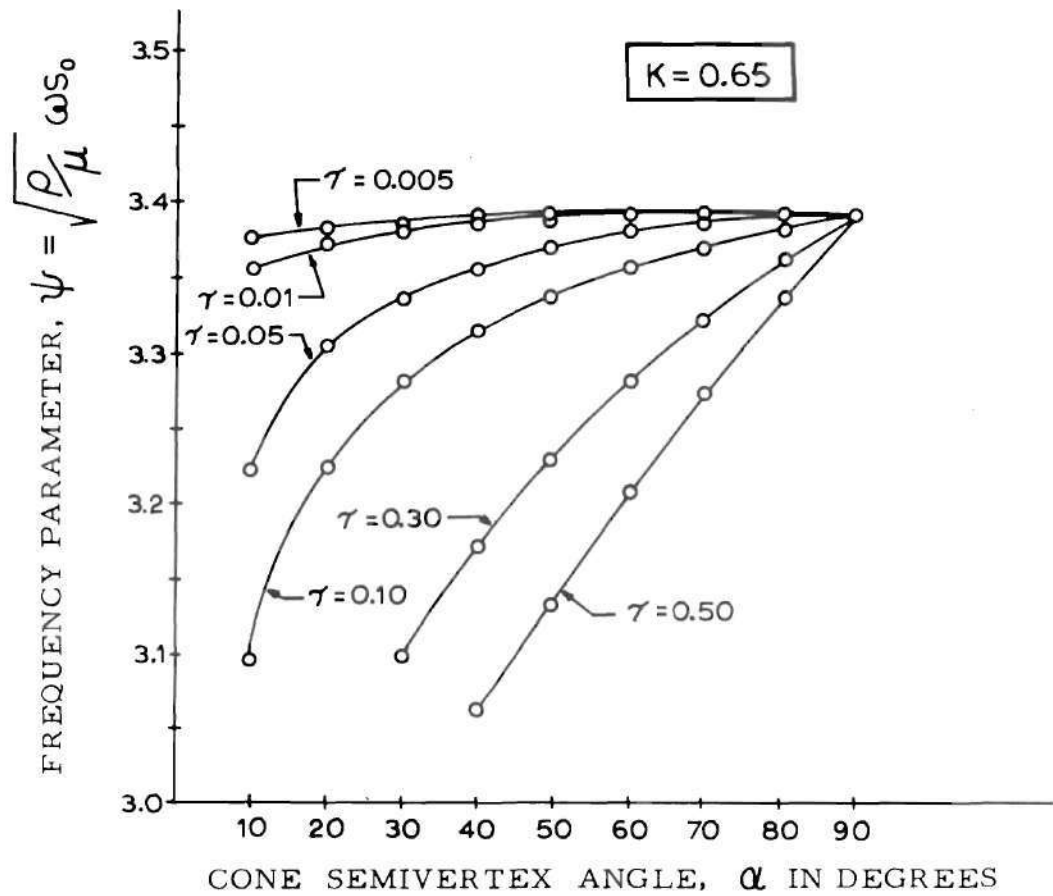


Figure 5 Frequency Parameter (ψ) Vs. Cone Semivertex Angle (α) For Different Thickness Parameters (τ). Cone Completeness Parameter (K) = 0.65

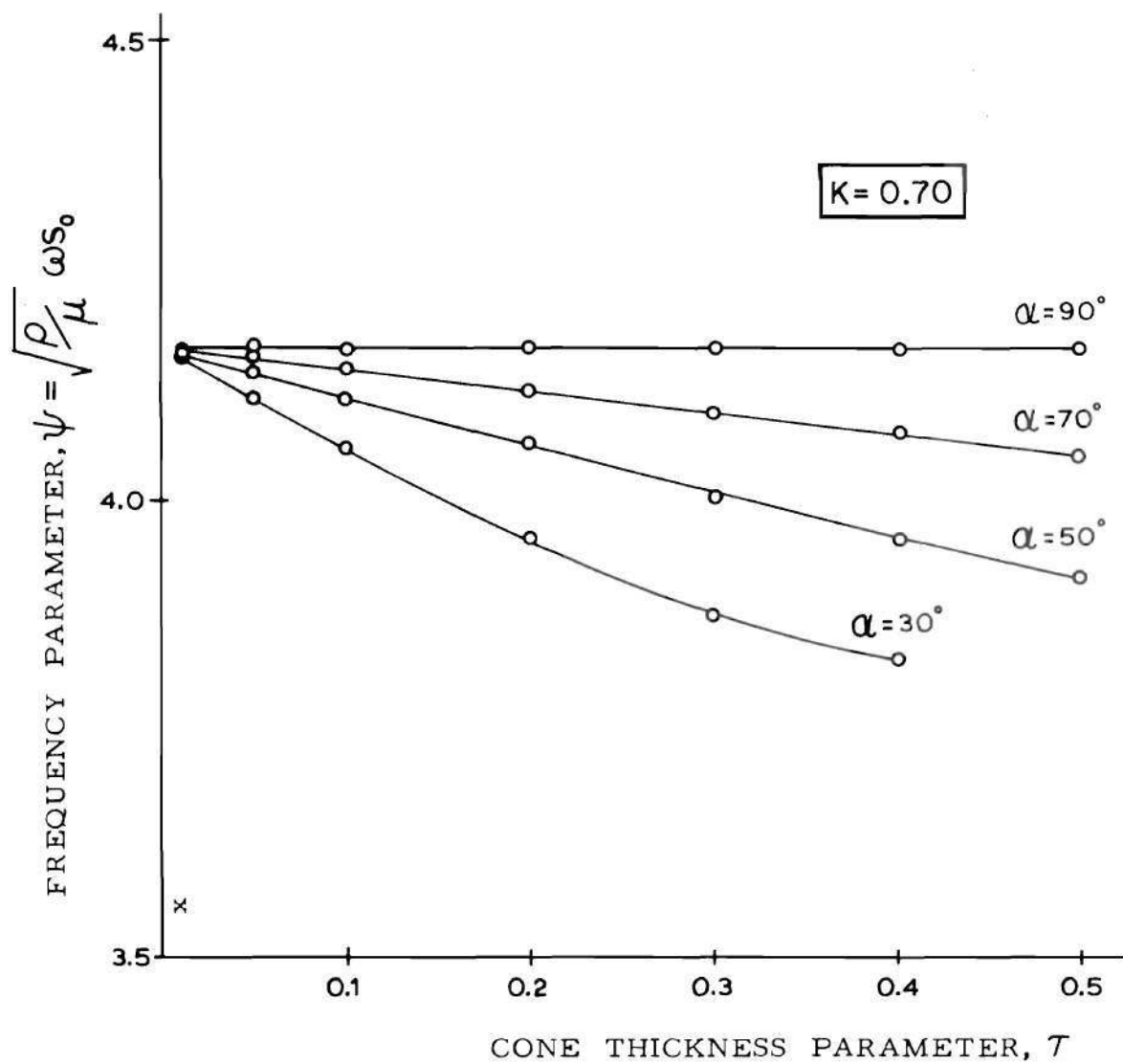


Figure 6 Frequency Parameter (ψ) Vs. Cone Thickness Parameter (τ) For Different Cone Semivertex Angles (α). Cone Completeness Parameter (K) = 0.70

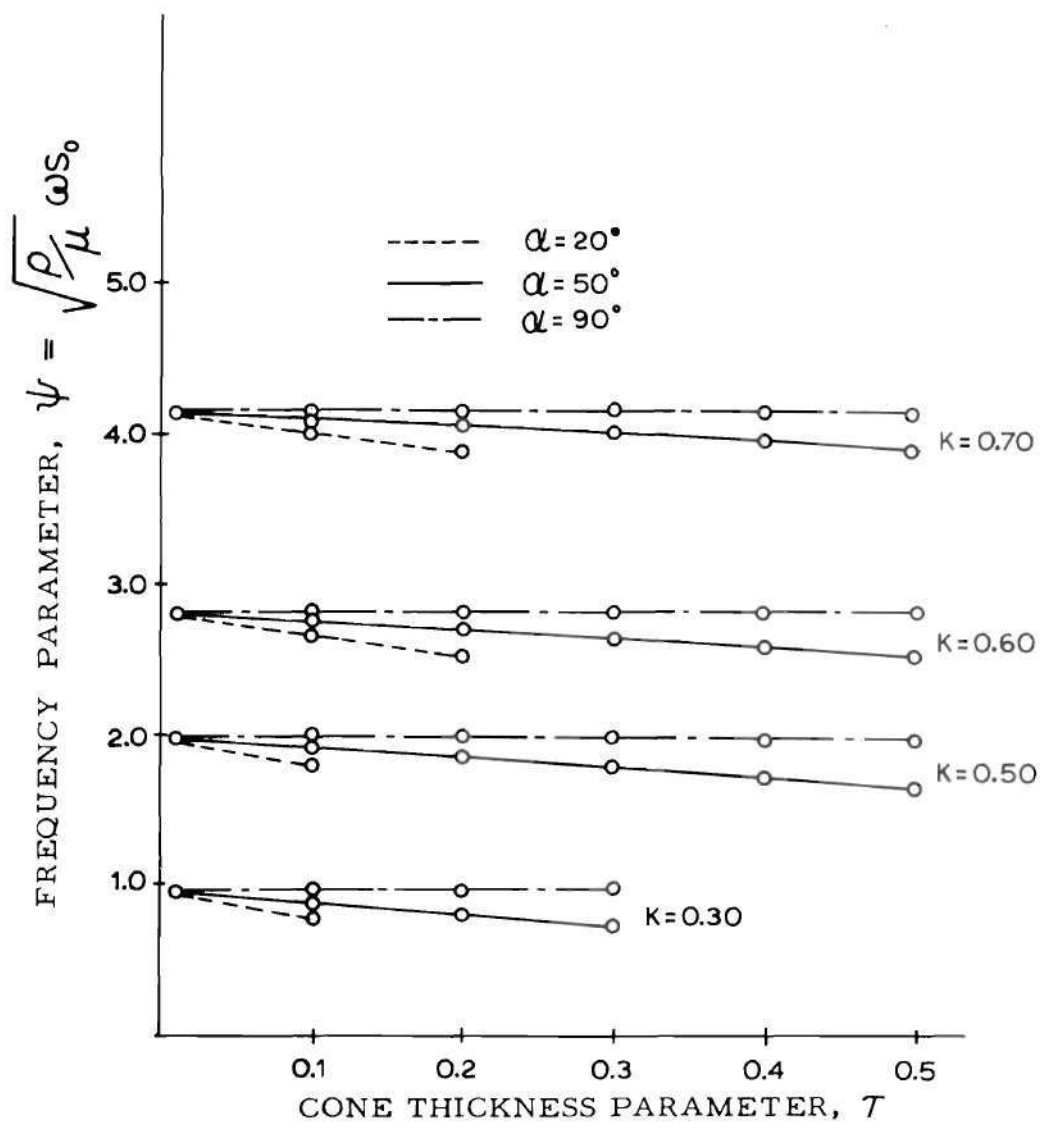


Figure 7 Frequency Parameter (ψ) Vs. Cone Thickness Parameter (τ) For Different Cone Completeness Parameters (K). Cone Semivertex Angle (α) = 20, 50 and 90 Degrees.

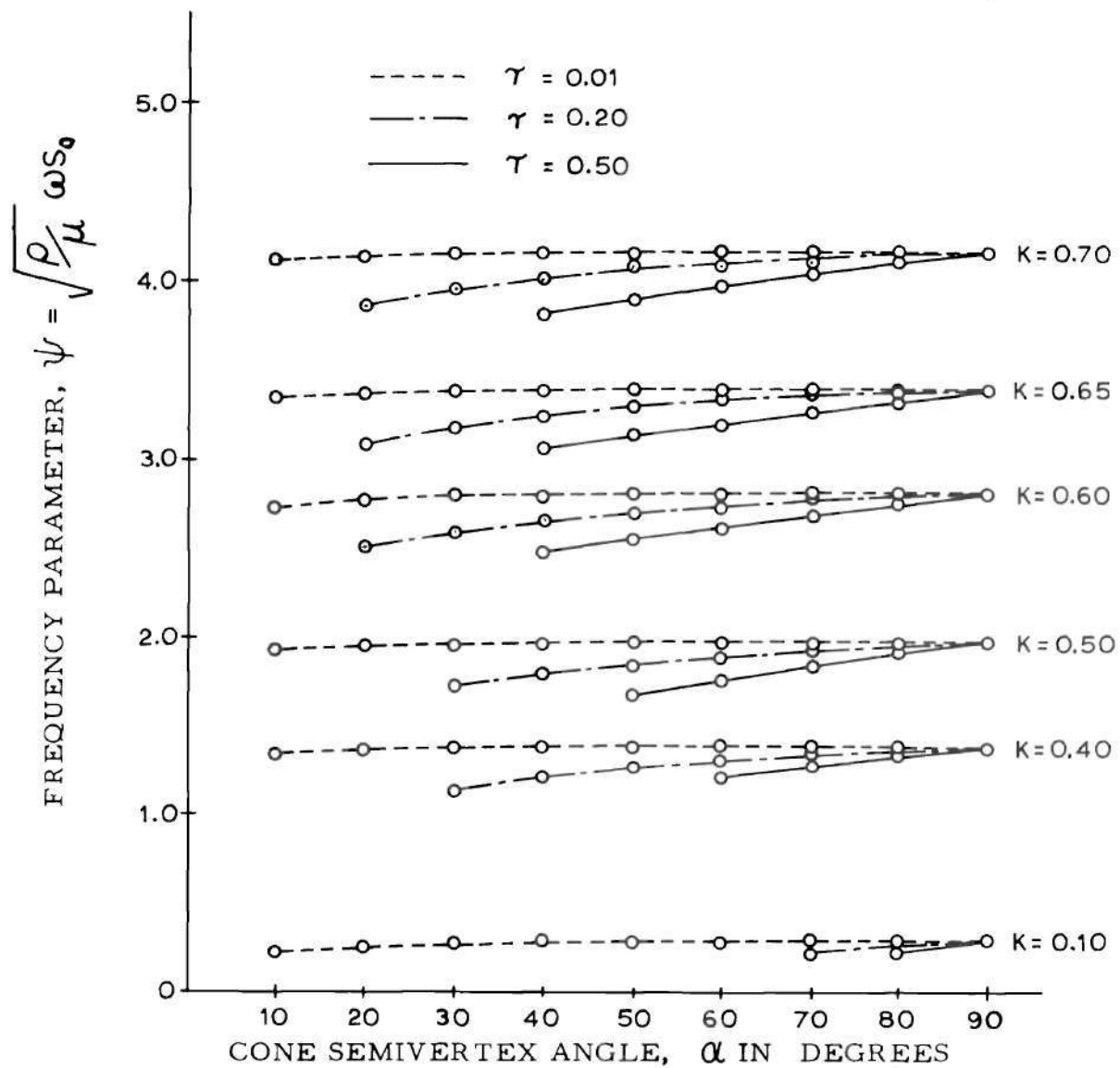


Figure 8 Frequency Parameter (ψ) Vs. Semivertex Angle (α) For Different Cone Completeness Parameters (K). Cone Thickness Parameters (τ) = 0.01, 0.20 and 0.50

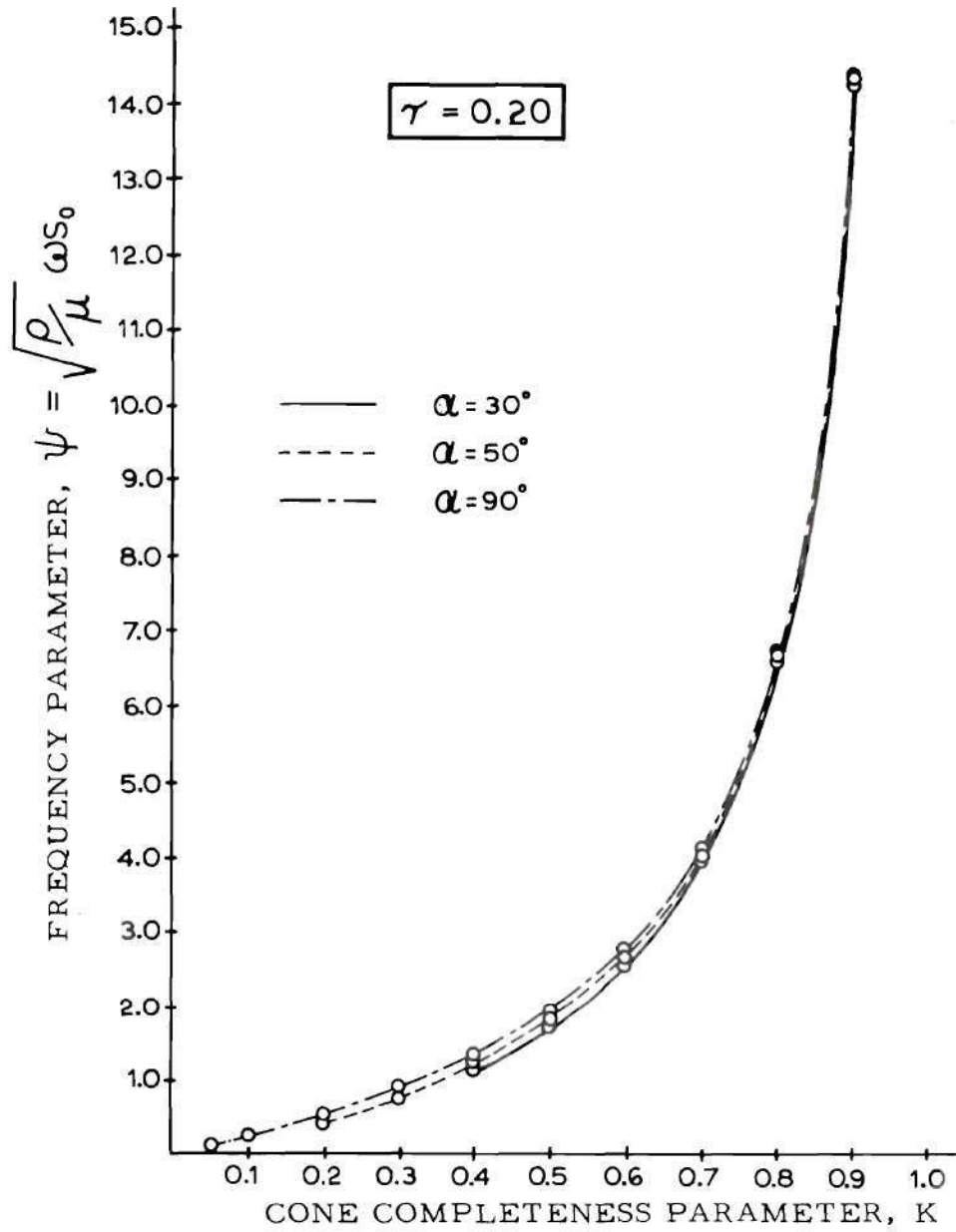


Figure 9 Frequency Parameter (ψ) Vs. Cone Completeness Parameter (K) For Different Semivertex Angles (α). Cone Thickness Parameter (τ) = 0.20

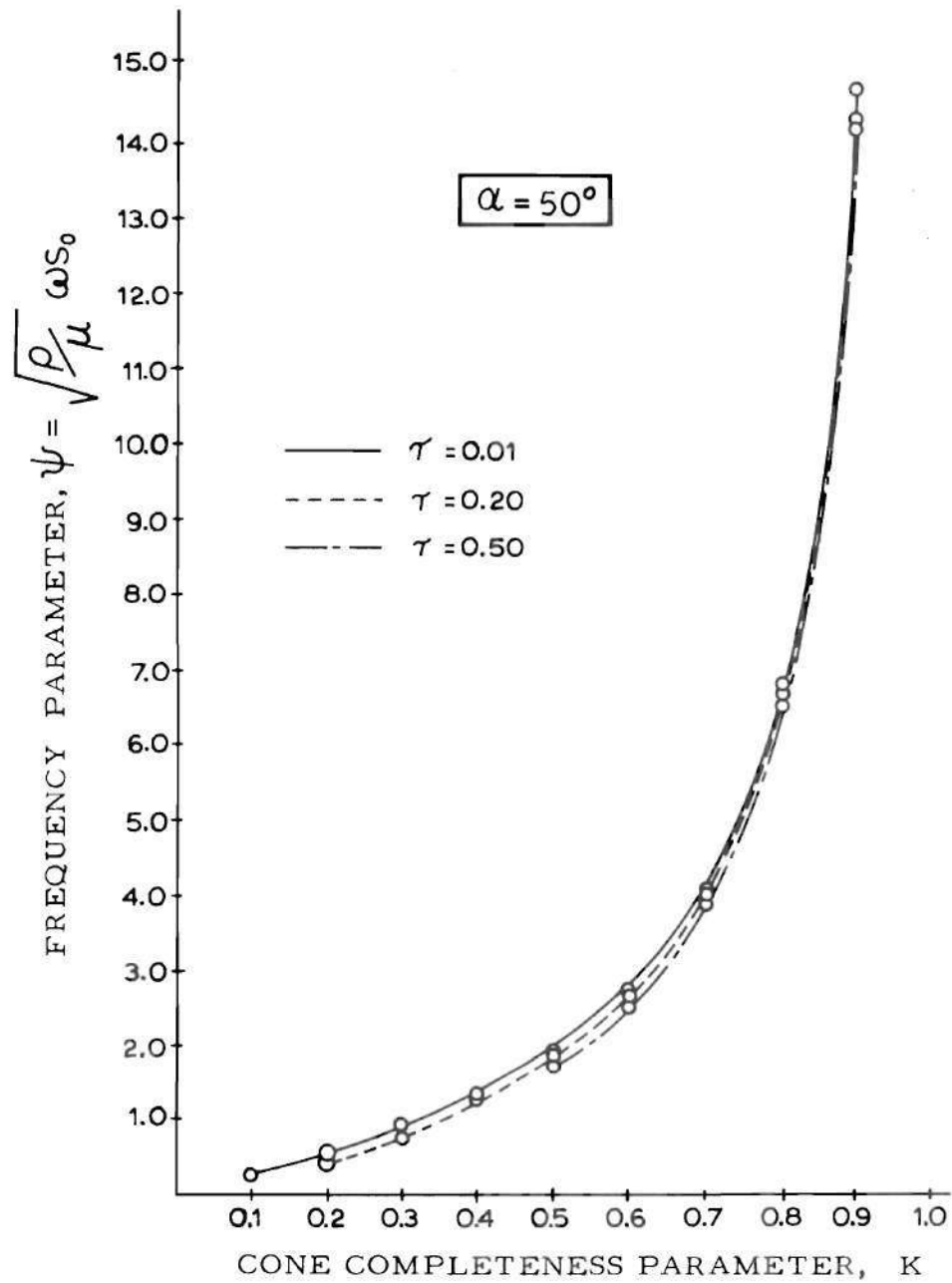


Figure 10

Frequency Parameter (ψ) Vs. Cone Completeness Parameter (K) For Different Thickness Parameters (τ). Cone Semivertex Angle (α) = 50 Degrees

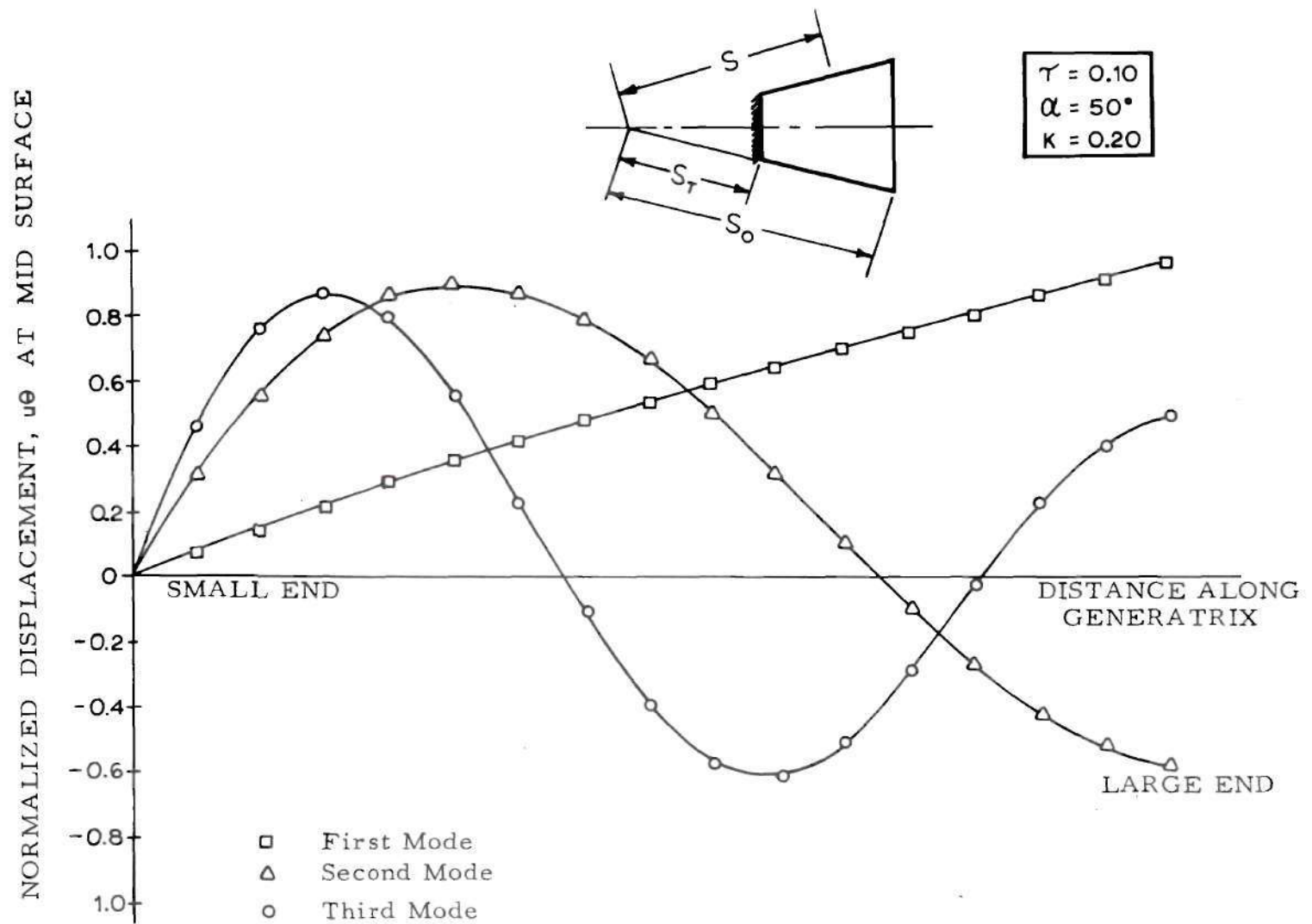


FIGURE 11 Torsional Mode Shapes For The Frustum Of A Cone

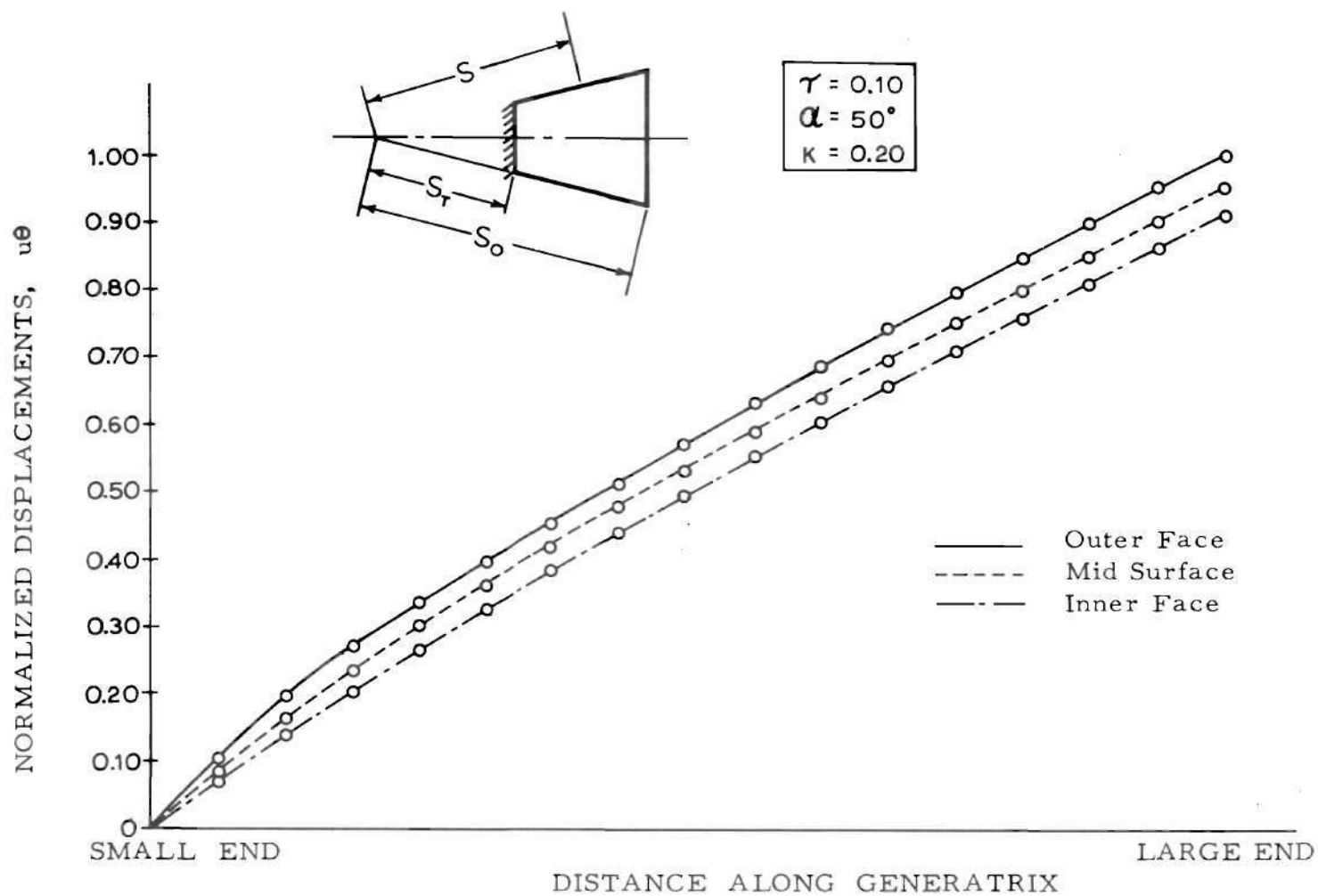


Figure 12 Variation of The Normalized Displacements Along The Thickness Of The Cone For The First Mode

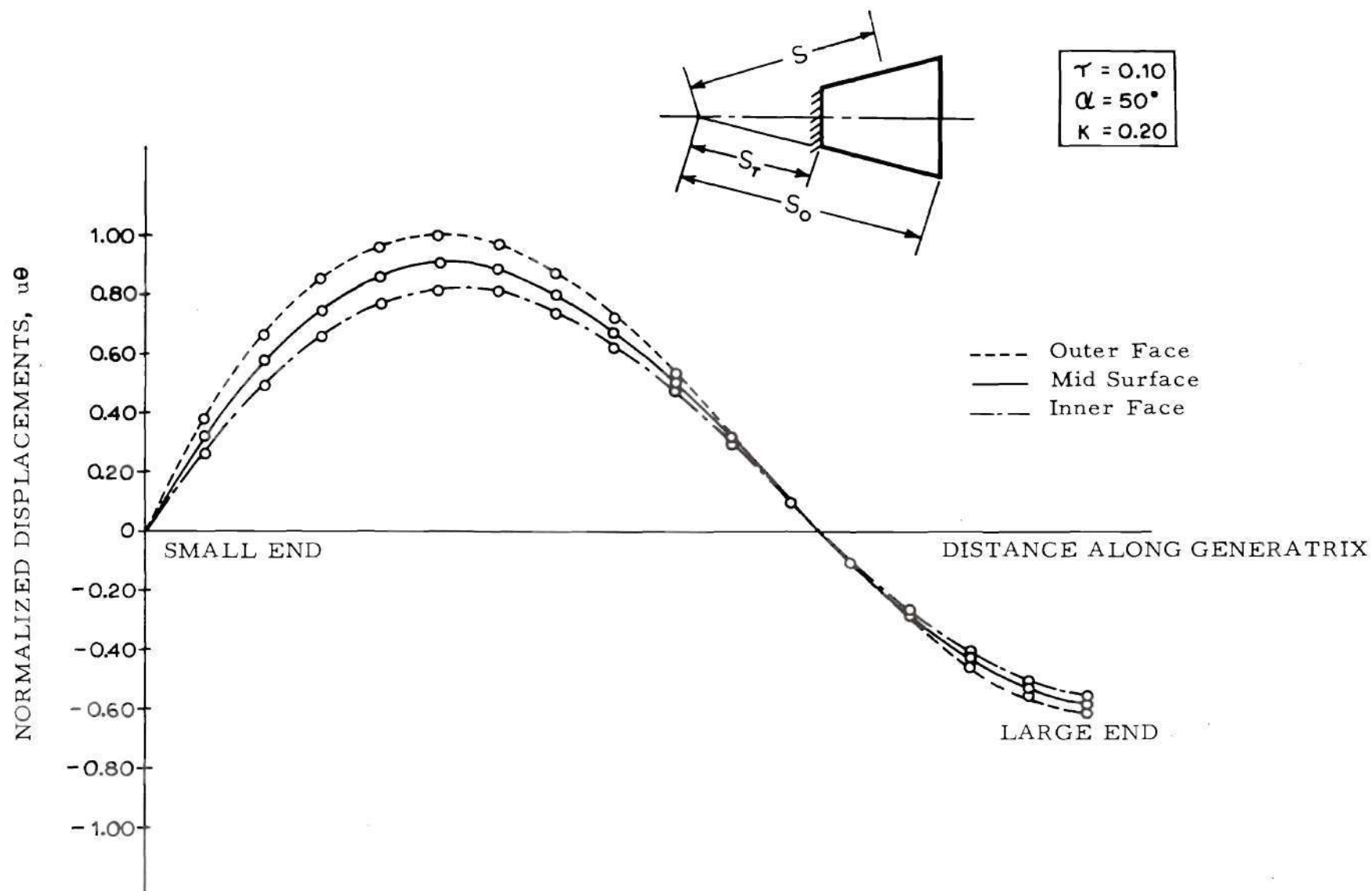


Figure 13 Variation Of The Normalized Displacements Along The Thickness Of The Cone For The Second Mode

RECOMMENDATIONS

The problem studied is the axisymmetric free torsional vibrations of a thick, hollowed, conical frustum which is fixed at the small end and free at the large end. The existing computer program can be modified and extended to study the effect of different boundary conditions and various types of loads, causing both static displacements and forced vibrations. Another logical extension of the present work would be to study the bending vibrational characteristics of truncated cones using the finite difference technique. The present study should also be extended to study vibrational characteristics of anisotropic, laminated shells. Shells of this construction are becoming more prevalent in space vehicles. Analytical techniques for their analyses, with experimental verification, have not kept pace with the present and future expected usage of composite shells.

APPENDIX A

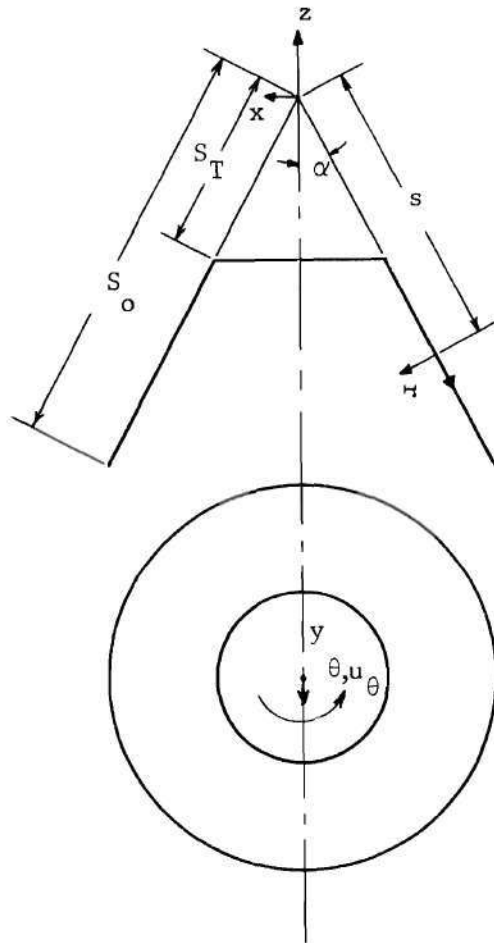
DERIVATION OF EQUATIONS OF MOTION
IN ORTHOGONAL CONICAL COORDINATES

Figure 14. Coordinate System.

The relationship between (x,y,z) and (s,r,θ) coordinates is given by

$$\left. \begin{aligned} x &= (s \sin \alpha - r \cos \alpha) \cos \theta \\ y &= (s \sin \alpha - r \cos \alpha) \sin \theta \\ z &= - (s \cos \alpha + r \sin \alpha) \end{aligned} \right\} \quad . \quad (A1)$$

The dimensional relationship between (s,r,θ) and (x,y,z) coordinate systems is given by h_s , h_r and h_θ called Lamé parameters.

The three parameters h_s , h_r and h_θ are obtained from the following expressions:

$$\left. \begin{aligned} h_s &= \sqrt{\left(\frac{\partial x}{\partial s}\right)^2 + \left(\frac{\partial y}{\partial s}\right)^2 + \left(\frac{\partial z}{\partial s}\right)^2} \\ h_r &= \sqrt{\left(\frac{\partial x}{\partial r}\right)^2 + \left(\frac{\partial y}{\partial r}\right)^2 + \left(\frac{\partial z}{\partial r}\right)^2} \\ h_\theta &= \sqrt{\left(\frac{\partial x}{\partial \theta}\right)^2 + \left(\frac{\partial y}{\partial \theta}\right)^2 + \left(\frac{\partial z}{\partial \theta}\right)^2} \end{aligned} \right\} \quad . \quad (A2)$$

In this particular set of coordinates,

$$\left. \begin{aligned} h_s &= h_r = 1 \\ h_\theta &= s \sin \alpha - r \cos \alpha \end{aligned} \right\} \quad . \quad (A3)$$

Let

$$\vec{u} = u_s \vec{e}_s + u_r \vec{e}_r + u_\theta \vec{e}_\theta \quad (A4)$$

where \vec{e}_s , \vec{e}_r and \vec{e}_θ are unit vectors in s, r and θ directions respectively.

The following relationships exist,

$$\left. \begin{aligned} \frac{\partial \vec{e}_s}{\partial s} &= \frac{\partial \vec{e}_r}{\partial s} = \frac{\partial \vec{e}_\theta}{\partial s} = 0 \\ \frac{\partial \vec{e}_s}{\partial r} &= \frac{\partial \vec{e}_r}{\partial r} = \frac{\partial \vec{e}_\theta}{\partial r} = 0 \\ \frac{\partial \vec{e}_s}{\partial \theta} &= \sin \alpha \vec{e}_\theta \\ \frac{\partial \vec{e}_r}{\partial \theta} &= -\cos \alpha \vec{e}_\theta \\ \frac{\partial \vec{e}_\theta}{\partial \theta} &= -\sin \alpha \vec{e}_s + \cos \alpha \vec{e}_r \end{aligned} \right\} . \quad (A5)$$

Now,

$$\begin{aligned} (\nabla \cdot \vec{u}) &= \text{div } \vec{u} \\ &= \frac{1}{h_s h_r h_\theta} \left[\frac{\partial}{\partial s} (h_r h_\theta u_s) + \frac{\partial}{\partial r} (h_s h_\theta u_r) + \frac{\partial}{\partial \theta} (h_r h_s u_\theta) \right] \end{aligned} \quad (A6)$$

$$\begin{aligned} \nabla(\nabla \cdot \vec{u}) &= \text{grad div } \vec{u} \\ &= \frac{1}{h_s} \frac{\partial}{\partial s} (\nabla \cdot \vec{u}) \vec{e}_s + \frac{1}{h_r} \frac{\partial}{\partial r} (\nabla \cdot \vec{u}) \vec{e}_r + \frac{1}{h_\theta} \frac{\partial}{\partial \theta} (\nabla \cdot \vec{u}) \vec{e}_\theta \end{aligned} \quad (A7)$$

$$\nabla^2 \vec{u} = \frac{1}{h_s h_r h_\theta} \left[\frac{\partial}{\partial s} \left(\frac{h_r h_\theta}{h_s} \frac{\partial \vec{u}}{\partial s} \right) + \frac{\partial}{\partial r} \left(\frac{h_s h_\theta}{h_r} \frac{\partial \vec{u}}{\partial r} \right) + \frac{\partial}{\partial \theta} \left(\frac{h_r h_s}{h_\theta} \frac{\partial \vec{u}}{\partial \theta} \right) \right] . \quad (A8)$$

APPENDIX B

DERIVATION OF RELATIONSHIPS BETWEEN STRESSES
AND DISPLACEMENTS IN ORTHOGONAL CONICAL COORDINATES

If the material is assumed to be homogeneous, isotropic and linearly elastic, then stresses in terms of strains are given by Hooke's law and are

$$\sigma_{ij} = 2\mu\epsilon_{ij} + \lambda\epsilon_{kk}\delta_{ij} \quad (B1)$$

where

σ_{ij} = stress tensor components

ϵ_{ij} = strain tensor components

λ, μ = Lamé constants

$$\epsilon_{kk} = \sum_{i=1}^{i=3} \epsilon_{ii} = \epsilon_{ss} + \epsilon_{rr} + \epsilon_{\theta\theta}$$

$$\delta_{ij} = \text{Kronecker delta i.e., } \delta_{ij} = \begin{cases} 1 & \text{for } i=j \\ 0 & \text{for } i \neq j \end{cases}$$

For the case of small deformations, the relationship between strain components and displacements in an orthogonal conical coordinate system is

$$\epsilon_{ss} = \frac{u_{s,s}}{h_s} + \left(\frac{u_r}{h_s h_r} \right) h_{s,r} + \left(\frac{u_\theta}{h_s h_\theta} \right) h_{s,\theta} \quad (B2)$$

$$\left. \begin{aligned}
 \epsilon_{rr} &= \frac{u_{r,r}}{h_r} + \left(\frac{u_s}{h_s h_r} \right) h_{r,s} + \left(\frac{u_\theta}{h_r h_\theta} \right) h_{r,\theta} \\
 \epsilon_{\theta\theta} &= \frac{u_{\theta,\theta}}{h_\theta} + \left(\frac{u_r}{h_r h_\theta} \right) h_{\theta,r} + \left(\frac{u_s}{h_s h_\theta} \right) h_{\theta,s} \\
 \epsilon_{rs} &= \frac{1}{2} \left[\frac{h_s}{h_r} \left(\frac{u_s}{h_s} \right)_{,r} + \frac{h_r}{h_s} \left(\frac{u_r}{h_r} \right)_{,s} \right] \\
 \epsilon_{r\theta} &= \frac{1}{2} \left[\frac{h_\theta}{h_r} \left(\frac{u_\theta}{h_\theta} \right)_{,r} + \frac{h_r}{h_\theta} \left(\frac{u_r}{h_r} \right)_{,\theta} \right] \\
 \epsilon_{\theta s} &= \frac{1}{2} \left[\frac{h_s}{h_\theta} \left(\frac{u_s}{h_s} \right)_{,\theta} + \frac{h_\theta}{h_s} \left(\frac{u_\theta}{h_\theta} \right)_{,s} \right]
 \end{aligned} \right\} \quad (B2)$$

The values of h_s , h_r and h_θ for the orthogonal conical coordinates are given in equation (A7) and are

$$h_s = h_r = 1$$

$$h_\theta = s \sin \alpha - r \cos \alpha$$

Substitution of the above values of h_s , h_r and h_θ in equations (B2) yields the expressions for the six strain components in orthogonal conical coordinates.

$$\left. \begin{aligned}
 \epsilon_{ss} &= u_{s,s} \\
 \epsilon_{rr} &= u_{r,r}
 \end{aligned} \right\} \quad (B3)$$

$$\left. \begin{aligned}
 \epsilon_{\theta\theta} &= \frac{1}{h_\theta} (u_s \sin\alpha - u_r \cos\alpha + u_{\theta,\theta}) \\
 \epsilon_{rs} &= \frac{1}{2} (u_{s,r} + u_{r,s}) \\
 \epsilon_{r\theta} &= \frac{1}{2} \left(u_{\theta,r} + \frac{u_\theta \cos\alpha}{h_\theta} + \frac{u_{r,\theta}}{h_\theta} \right) \\
 \epsilon_{\theta s} &= \frac{1}{2} \left(u_{\theta,s} - \frac{u_\theta \sin\alpha}{h_\theta} + \frac{u_{s,\theta}}{h_\theta} \right)
 \end{aligned} \right\} \quad (B3)$$

Stresses in terms of displacements are obtained by substitution in equation (B1), the expressions for strains obtained in equations (B3).

Then expression for stresses are

$$\left. \begin{aligned}
 \sigma_{ss} &= (2\mu + \lambda)u_{s,s} + \lambda \left(u_{r,r} + \frac{u_s \sin\alpha}{h_\theta} - \frac{u_r \cos\alpha}{h_\theta} + \frac{u_{\theta,\theta}}{h_\theta} \right) \\
 \sigma_{rr} &= (2\mu + \lambda)u_{r,r} + \lambda \left(u_{s,s} + \frac{u_s \sin\alpha}{h_\theta} - \frac{u_r \cos\alpha}{h_\theta} + \frac{u_{\theta,\theta}}{h_\theta} \right) \\
 \sigma_{\theta\theta} &= (2\mu + \lambda) \left(\frac{u_s \sin\alpha}{h_\theta} - \frac{u_r \cos\alpha}{h_\theta} + \frac{u_{\theta,\theta}}{h_\theta} \right) + \lambda (u_{s,s} + u_{r,r}) \\
 \sigma_{rs} &= \mu (u_{s,r} + u_{r,s}) \\
 \sigma_{r\theta} &= \mu \left(u_{\theta,r} + \frac{u_\theta \cos\alpha}{h_\theta} + \frac{u_{r,\theta}}{h_\theta} \right) \\
 \sigma_{\theta s} &= \mu \left(u_{\theta,s} - \frac{u_\theta \sin\alpha}{h_\theta} + \frac{u_{s,\theta}}{h_\theta} \right)
 \end{aligned} \right\} \quad (B4)$$

Expressions for stresses and strains for the axisymmetric case can be obtained from the corresponding general equations by dropping the terms involving derivatives with respect to θ .

APPENDIX C

DERIVATION OF BOUNDARY CONDITIONS

The boundary conditions for the problem are derived using a variational procedure.

The total work of deformation U , is given by

$$U = \int_{\text{volume}} \varphi \, dv . \quad (C1)$$

Where

φ = strain energy of deformation per unit volume

dv = differential volume of an element.

Strain energy of deformation per unit volume, φ is equal to $\frac{1}{2} \sigma_{ij} \epsilon_{ij}$ in which σ_{ij} and ϵ_{ij} are stress and strain tensor components respectively.

Expressions for σ_{ij} and ϵ_{ij} are given in equations (B3) and (B4) of Appendix B.

The differential volume of an element in an orthogonal coordinate system is given by

$$dv = h_s h_r h_\theta ds dr d\theta . \quad (C2)$$

As shown in equation (A4) of Appendix A, $h_s = h_r = 1$ and $h_\theta = s \sin \alpha - r \cos \alpha$.

Then

$$dv = h_{\theta} ds dr d\theta .$$

Then the expression for strain energy of deformation in the present orthogonal conical coordinate system is

$$\begin{aligned} U = \frac{1}{2} \int_{\text{volume}} & (\sigma_{ss}\epsilon_{ss} + \sigma_{rr}\epsilon_{rr} + \sigma_{\theta\theta}\epsilon_{\theta\theta} + \sigma_{rs}\epsilon_{rs} \\ & + \sigma_{r\theta}\epsilon_{r\theta} + \sigma_{s\theta}\epsilon_{s\theta}) h_{\theta} ds dr d\theta . \end{aligned} \quad (C3)$$

The technique of obtaining the equations of motion and boundary conditions using the variational procedure is shown in detail using the stress $\sigma_{r\theta}$ and its corresponding strain $\epsilon_{r\theta}$.

From equations (B3) and (B4) of Appendix B

$$\epsilon_{r\theta} = \frac{1}{2} \left(u_{\theta,r} + \frac{u_{\theta} \cos \alpha}{h_{\theta}} + \frac{u_{r,\theta}}{h_{\theta}} \right) \quad (C4)$$

$$\sigma_{r\theta} = \mu \left(u_{\theta,r} + \frac{u_{\theta} \cos \alpha}{h_{\theta}} + \frac{u_{r,\theta}}{h_{\theta}} \right) \quad (C5)$$

Then total strain energy of deformation, $U_{r\theta}$ due to stress $\sigma_{r\theta}$ and strain $\epsilon_{r\theta}$ is

$$\begin{aligned} U_{r\theta} &= \frac{1}{2} \int_{\text{volume}} \sigma_{r\theta} \epsilon_{r\theta} \\ &= \frac{\mu}{4} \iiint_{sr\theta} \left(u_{\theta,r} + \frac{u_{\theta} \cos \alpha}{h_{\theta}} + \frac{u_{r,\theta}}{h_{\theta}} \right)^2 h_{\theta} ds dr d\theta . \end{aligned} \quad (C6)$$

Taking the first variation yields

$$\begin{aligned} \delta U_{r\theta} = & \frac{\mu}{2} \iiint_{sr\theta} \left(u_{\theta,r} + \frac{u_{\theta} \cos \alpha}{h_{\theta}} + \frac{u_{r,\theta}}{h_{\theta}} \right) \left(\delta(u_{\theta,r}) + \delta \left(\frac{u_{\theta} \cos \alpha}{h_{\theta}} \right) \right. \\ & \left. + \delta \left(\frac{u_{r,\theta}}{h_{\theta}} \right) \right) h_{\theta} ds dr d\theta . \end{aligned} \quad (C7)$$

Using integration by parts, the above equation becomes

$$\begin{aligned} \delta U_{r\theta} = & \frac{\mu}{2} \iiint_{sr\theta} \left(u_{\theta,r} + \frac{u_{\theta} \cos \alpha}{h_{\theta}} + \frac{u_{r,\theta}}{h_{\theta}} \right) h_{\theta} \delta u_{\theta} \Big|_{r \text{ limits}} ds d\theta \\ & - \frac{\mu}{2} \iiint_{sr\theta} \left[h_{\theta} \left(u_{\theta,rr} + \frac{\cos \alpha}{h_{\theta}} u_{\theta,r} + \frac{u_{r,\theta r}}{h_{\theta}} \right) - \cos \alpha u_{\theta,r} \right] \delta u_{\theta} ds dr d\theta \\ & + \frac{\mu}{2} \iiint_{sr\theta} \cos \alpha \left(u_{\theta,r} + \frac{u_{\theta} \cos \alpha}{h_{\theta}} + \frac{u_{r,\theta}}{h_{\theta}} \right) \delta u_{\theta} ds dr d\theta \\ & + \frac{\mu}{2} \iiint_{sr} \left(u_{\theta,r} + \frac{u_{\theta} \cos \alpha}{h_{\theta}} + \frac{u_{r,\theta}}{h_{\theta}} \right) \delta u_r \Big|_{\theta \text{ limits}} ds dr \\ & - \frac{\mu}{2} \iiint_{sr\theta} \left(u_{\theta,r\theta} + \frac{\cos \alpha}{h_{\theta}} u_{\theta,\theta} + \frac{u_{r,\theta\theta}}{h_{\theta}} \right) \delta u_r ds dr d\theta . \end{aligned} \quad (C8)$$

Similar expressions can be obtained by taking variation of strain energy due to other stresses.

Then the boundary conditions for the torsional vibrations can be obtained by collecting area integral terms involving variation with respect to u_{θ} . These terms when grouped by the same boundaries becomes

r limits

$$\frac{\mu}{2} \iint_{s\theta} h_{\theta} \left(u_{\theta,r} + \frac{u_{\theta} \cos \alpha}{h_{\theta}} + u_{r,\theta} \right) \Big|_{r \text{ limits}} ds d\theta \quad (C9)$$

s limits

$$\frac{\mu}{2} \iint_{r\theta} h_{\theta} \left(\frac{u_{s,\theta}}{h_{\theta}} - \frac{u_{\theta} \sin \alpha}{h_{\theta}} + u_{\theta,s} \right) \Big|_{s \text{ limits}} dr d\theta \quad (C10)$$

\theta limits

$$\iint_{rs} \left[(2\mu + \lambda) \left(\frac{u_s \sin \alpha}{h_{\theta}} - \frac{u_r \cos \alpha}{h_{\theta}} + \frac{u_{\theta,\theta}}{h_{\theta}} \right) + \lambda (u_{s,s} + u_{r,r}) \right] \Big|_{\theta \text{ limits}} dr ds \quad (C11)$$

Using equations of (B4) in appendix, the above expressions can be written as

r limits

$$\frac{1}{2} \iint_{s\theta} h_{\theta} \sigma_{r\theta} \Big|_{r \text{ limits}} ds d\theta \quad (C12)$$

s limits

$$\frac{1}{2} \iint_{r\theta} h_{\theta} \sigma_{\theta s} \Big|_{s \text{ limits}} dr d\theta \quad (C13)$$

\theta limits

$$\iint_{rs} \sigma_{\theta\theta} \Big|_{\theta \text{ limits}} dr ds \quad (C14)$$

Expressions (C12), (C13) and (C14) are equal to zero for the free vibrations. It may be noted that, collecting all volume integral terms involving first variation with respect to u_θ will give equation of motion in θ direction.

Similarly boundary conditions for flexural vibrations can be obtained and are as follows:

r limits

$$\iint_{s\theta} h_\theta \sigma_{rr} \Big|_{r \text{ limits}} ds d\theta \qquad \frac{1}{2} \iint_{s\theta} h_\theta \sigma_{rs} \Big|_{r \text{ limits}} ds d\theta \qquad (C15)$$

s limits

$$\frac{1}{2} \iint_{r\theta} h_\theta \sigma_{rs} \Big|_{s \text{ limits}} dr d\theta \qquad \iint_{r\theta} h_\theta \sigma_{ss} \Big|_{s \text{ limits}} dr d\theta \qquad (C16)$$

θ limits

$$\frac{1}{2} \iint_{rs} \sigma_{r\theta} \Big|_{\theta \text{ limits}} dr ds \qquad \frac{1}{2} \iint_{rs} \sigma_{\theta s} \Big|_{\theta \text{ limits}} dr ds \qquad (C17)$$

Expressions in (C15), (C16) and (C17) should be set equal to zero for free vibrations. Also terms having θ limits or expressions in equations (C14) and (C17) drop out for axisymmetric vibrations.

BIBLIOGRAPHY

1. Nash, W. A., "Bibliography on Shells and Shell-Like Structures," David W. Taylor Model Basin, Report No. 863, Nov. 1954.
2. Nash, W. A., "Bibliography on Shells and Shell-Like Structures," (1954-1956) Univ. of Florida, Dept. of Engineering Mechanics, June 1957.
3. Hu, W. C. L., "A Survey of the Literature on the Vibrations of Thin Shells," Southwest Research Institute, Project No. 02-1504, Technical Report No. 1, June 1964, NASA-N 64-27313.
4. Gros, C., and Forsberg, K., "Vibrations of Thin Shells: A Partially Annotated Bibliography," Lockheed Missiles and Space Company, Report No. 3-71-63-2 (SB-63-43), April 1963, NASA-N63-19776.
5. Hu, W. C. L., "Free Vibrations of Conical Shells," NASA-TN-D-2666, Feb. 1965, NASA-N65-17330.
6. Platus, D. H., "Conical Shell Vibrations, NASA-TN-D-2767, Feb. 1965, NASA-N65-22363.
7. Siede, P., "On the Free Vibrations of Simply Supported Conical Shells," TDR-269(4560-40)-2, Feb. 1964, NASA-N64-22318.
8. Federhofer, K., "Natural Vibrations of the Conical Shells, NASA TTF-8261, Nov. 1962, NASA N65-15351.
9. Hermann, G., and Mirsky, I., "On Vibrations of Conical Shells," Journal of the Aero/Space Sciences, Vol. 25, No. 7, July 1958, pp. 451-458.
10. Sanders, H., Wisniewski, E., and Paslay, P., "Vibrations of Conical Shells," Journal of the Acoustical Society of America, Vol. 32, No. 6, June 1960, pp. 765-772.
11. Weingarten, V., and Gelman, A., "Free Vibrations of Cantilevered Conical Shells," Journal of the Engineering Mechanics Division, ASCE, Vol. 93, No. EM6, Proc. Paper 5661, Dec. 1967, pp. 127-138.
12. Weingarten, V., "Free Vibrations of Conical Shells," Journal of the Engineering Mechanics Division, ASCE, Vol. 91, No. EM4, Proc. Paper 4440, August 1965, pp. 69-87.
13. Goldberg, J., Bogdanoff, J., and Marcus, L., "On the Calculation of the Axisymmetric Modes and Frequencies of Conical Shells,"

- Journal of the Acoustical Society of America, Vol. 32, No. 6, June 1960, pp. 738-742.
14. Garnet, H., and Kempner, J., "Axisymmetric Free Vibrations of Conical Shells," Journal of Applied Mechanics, Paper No. 64, APM-24, Vol. 31, Sept. 1964, pp. 458-465.
 15. Pshenichnov, G., "Free Axisymmetric Vibrations of Thin Elastic Shells of Revolution," NASA TT F-12787, April 1970, NASA-N70-25680.
 16. Watkins, J., and Clary, R., "Vibrational Characteristics of Some Thin-Walled Cylindrical and Conical Frustum Shells," NASA-TN-D-2729, March 1965, NASA-N65-19915.
 17. Kagawa, Y., "On the Axisymmetrical Vibrations of Conical Shells," Scientific Report No. 6, AFOSR-65-1422, June 1965, AD-627963.
 18. Krause, F., "Natural Frequencies and Mode Shapes of the Truncated Conical Shells with Free Edges," SAMSO-TR-68-37, January 1968, NASA-N68-20727.
 19. Garnet, H., Goldberg, M., and Salerno, V., "Torsional Vibrations of Shells of Revolution," Journal of Applied Mechanics, Vol. 28, Dec. 1961, pp. 571-573.
 20. Francis, J., "The Q-R Transformation," The Computer Journal, Vol. 4, No. 3, Oct. 1961, Vol. 4, No. 4, Jan. 1962.
 21. Wilkinson, J., The Algebraic Eigenvalue Problem, Clarendon Press, Oxford, 1965.
 22. McGill, D., "Axisymmetric Free Oscillations of Thick Toroidal Shells," Ph.D. Thesis, University of Kansas, June 1966.
 23. Novozhilov, V., Theory of Elasticity, Pergamon Press, New York, 1961.
 24. Salvadori, M., and Baron, M., Numerical Methods in Engineering, Prentice Hall, Inc., Englewood Cliffs, N. J., 1961.